Res Chem Intermed (2017) 43:1383–1394
DOI 10.1007/s11164-016-2704-7

Biosynthesis, characterization, and antimicrobial effect of silver nanoparticles obtained using *Lavandula* × *intermedia*

Elias E. Elemike[1,2,3] · Damian C. Onwudiwe[1,2] · Anthony C. Ekennia[4] · Lebogang Katata-Seru[1,2]

Received: 24 May 2016 / Accepted: 12 August 2016 / Published online: 24 August 2016

Abstract The use..... of aqueous leaf extract of *Lavandula* × *intermedia* for biosynthesis of silver nanoparticles (AgNPs) is presented. The plant extract was obtained by boiling dried leaves and using the obtained filtrate for the synthesis of AgNPs. The study was conducted to investigate an ecofriendly approach to metal nanoparticle synthesis and to evaluate the antimicrobial potential of both the aqueous plant extract and resulting silver nanoparticles against different microbes using the disc diffusion method. The synthesis of silver nanoparticles was monitored using ultraviolet–visible (UV–v is) spectroscopy, which showed a localized surface plasmon resonance band at 411 nm and a shift of the band to higher wavenumber of 422 nm after 90 min of reaction. Powder X-ray diffraction analysis and transmission electron microscopy of the obtained AgNPs revealed their crystalline nature, with average size of 12.6 nm. Presence of elemental silver was further confirmed by energy-dispersive X-ray spectroscopy. Fourier-transform infrared spectroscopy confirmed presence of phytochemicals from *Lavandula* × *intermedia* leaf extract on the AgNPs. The AgNPs showed good antimicrobial activity with inhibition zone ranging from 10 to 23 mm; the largest inhibition zone (23 mm) occurred against

✉ Damian C. Onwudiwe
Damian.Onwudiwe@nwu.ac.za

[1] Material Science Innovation and Modelling (MaSIM) Research Focus Area, Faculty of Agriculture, Science and Technology, North-West University, Mafikeng Campus, Private Bag X2046, Mmabatho 2735, South Africa

[2] Department of Chemistry, School of Mathematics and Physical Sciences, Faculty of Agriculture, Science and Technology, North-West University, Mafikeng Campus, Private Bag X2046, Mmabatho 2375, South Africa

[3] Department of Chemistry, College of Science, Federal University of Petroleum Resources, P.M.B. 1221, Effurun, Delta State, Nigeria

[4] Department of Chemistry, Federal University, Ndufu-Alike Ikwo (FUNAI), P.M.B. 1010, Abakaliki, Ebonyi State, Nigeria

Escherichia coli. Generally, the AgNPs displayed more antimicrobial activity against all investigated pathogens compared with *Lavandula* × *intermedia* leaf extract, and were also more active than streptomycin against *Klebsiella oxytoca* and *E. coli* at the same concentration. The silver nanoparticles showed prominent antimicrobial activity with a lowest minimum inhibitory concentration (MIC) value of 15 μg/mL against *E. coli*, *K. oxytoca*, and *Candida albicans*.

Keywords Silver · Biosynthesis · Antimicrobial · *Lavandula* × *intermedia*

Introduction

Biosynthesis of nanoparticles involves use of plant extracts or microorganisms for reduction of macromolecular particles to nanosized forms [1, 2]. However, such microorganism-mediated biosynthesis of nanoparticles involves a long process of culturing, strain isolation, and screening [3, 4]. Use of extracts from various plants in biosynthesis of nanoparticles is a simpler, ecofriendly, and important reaction route in the field of green nanochemistry [1, 2]. The effectiveness of this method is due to the fact that some constituent bioactive secondary metabolites such as terpenoids, flavonoids, phenolics, carbonyl compounds, and alkaloids in plants have reducing and stabilizing properties that can be utilized in biosynthesis of nanosized materials. Similarly, plant-mediated biosynthesis of nanoparticles is another route to form metal nanoclusters (NCs), which are emerging as a new class of functional nanomaterials in the areas of biological sensing, labeling, imaging, and therapy due to their unique physical and chemical properties, such as ultrasmall size, highest occupied molecular orbital (HOMO)–lowest unoccupied molecular orbital (LUMO) transition, and strong luminescence, together with good photostability and biocompatibility [5].

Several types of nanoparticles have been reported as products of bioreduction processes using different plant extracts. Recently, AgNPs synthesized using extracts of melon [6], *Coffea arabica* [7], *Averrhoa carambola* [8], *Skimmia laureola* [9], *Diospyros paniculata* [10], *Tamarix gallica* [11], *Clerodendrum serratum* [12], *Prosopis farcta* [13], *Rosmarinus officinalis* [14], etc. have been reported.

The plant used in this study, *Lavandula* × *intermedia*, belongs to the Lamiaceae family, which includes numerous medicinal herbs with pronounced therapeutic properties [15]. The species of *Lavandula* are aromatic plants, mainly distributed in the Mediterranean area. Medicinal uses of lavender inflorescence are based on its sedative, cholagogue, spasmolytic, carminative, and antiseptic properties [15]. *Lavandula* species are also grown for their wide range of uses in perfumery, cosmetics, and food processing. Previous phytochemical studies have indicated that *Lavandula* species contain essential oil, triterpenes, coumarins, hydroxycinnamic acids, and flavonoids [16]. Lavandin was originally produced to serve as a raw material to obtain essential oils with yield five times higher than that of *L. angustifolia*. *Lavandula* × *intermedia* (lavandin) is characterized by high 1,8-cineole (eucalyptol), camphor, linalool, borneol, and linalyl acetate content, denoting low oil quality according to perfumery standards, but of interesting value

as medicinal oil [17, 18]. Previous studies have reported the antimicrobial activities of several essential oil isolates [19–21] and nonvolatile extracts [22] of *Lavandula* × *intermedia* against some pathogens.

The number of invasive and systemic pathogenic infections has increased dramatically due to the growing number of immunocompromised patients as a result of cancer chemotherapy, organ transplantation, and human immunodeficiency virus (HIV) infection [23, 24]. Consequently, cases of drug resistance have become a growing concern in treatment of infectious diseases caused by bacteria and fungi [25]. Hence, discovery and development of effective antibacterial and antifungal drugs with novel mechanisms of action has become an urgent task for infectious disease research programs [26]. In view of the potential of AgNPs as effective antimicrobial agents [27], we report herein green synthesis of silver nanoparticles mediated by use of leaf extract of *Lavandula* × *intermedia*. The size and morphology of the nanosized particles were determined. The antimicrobial potential of the AgNPs against several pathogens was determined and compared with that of leaf extract of *Lavandula* × *intermedia* and positive control drugs.

Materials and methods

Preparation of aqueous leaf extract

Lavandula × *intermedia* leaves were collected, dried at room temperature, and ground using an electric grinder. Aqueous leaf extract was prepared according to literature [28]. Plant aqueous extract was prepared by mixing 1.60 g dried leaf with 200 mL distilled water and boiling for 60 min. The mixture was then filtered twice through 2-μm-pore sterile filter paper into a sterile tube and stored at 4 °C.

Preparation of LX-AgNPs

Biosynthesised nanoparticles were prepared following a reported literature procedure [29]. Aqueous leaf extract of *Lavandula* × *intermedia* (80 mL) was added to 400 mL 1 mM $AgNO_3$ and mixed on a magnetic stirrer at 90 °C with continuous stirring. The color of the mixture gradually changed to yellowish brown and further to dark brown, indicating formation of AgNPs. The gradual process of nanoparticle formation was monitored using UV–Vis spectroscopy at different time intervals. The resulting colloidal solution was centrifuged at 4000 rpm for 1 h, and the resulting nanoparticles were dried for further characterization.

Characterization of silver nanoparticles (LX-AgNPs)

The synthesis of AgNPs was monitored by sampling the reaction mixture at regular intervals and determining the absorption maximum using a UV-1901 UV–Vis spectrophotometer (Agilent Technology, Cary series, USA) at wavelength of 200–800 nm. X-ray diffraction (XRD) measurements were performed at voltage of 30 kV using Ni-filtered Cu K_α radiation at wavelength of 1.540587 nm using a

Röntgen PW3040/60 X'Pert Pro X-ray diffractometer. Fourier-transform infrared (FTIR) spectral measurements were conducted using a Cary 600 series FTIR spectrometer (Agilent Technology, USA), recording the spectrum at resolution of 4 cm^{-1}. The external and internal morphology of the nanoparticles was studied using a Quanta FEG 250 environmental scanning electron microscope (ESEM) and TECNAI G2 (ACI) transmission electron microscope, respectively. The presence of elemental silver was determined to check the surface interatomic distribution using energy-dispersive X-ray (EDX) spectroscopy.

Antimicrobial studies

Clinical isolates of different microbial strains were collected from the Department of Microbiology, University College Hospital, Ibadan, Nigeria. The bacterial strains were *Escherichia coli*, *Pseudomonas aeruginosa*, *Proteus mirabilis*, *Bacillus cereus*, *Klebsiella oxytoca*, *Salmonella typhi*, and *Staphylococcus aureus*. The fungal organisms were *Candida albicans*, *Aspergillus niger*, and *Fusarium oxysporum*. The microbial strains were chosen based on their clinical and pharmacological importance [30]. Antimicrobial screening was carried out using the agar disc diffusion method [29, 31] at the Department of Microbiology, University of Ibadan, Nigeria.

Petri plates were prepared using sterile Muller–Hinton agar (MHA). Inocula of test cultures were streaked onto condensed Muller–Hinton agar in Petri plates using a sterilized cotton swab to ensure a uniform thick lawn or growth layer, and allowed to dry for 15 min. AgNP stock solution with concentration of 100 μg/mL was prepared using 100 % dimethyl sulfoxide as diluent [32]. Stock solutions of plant extract and standard drugs were prepared using double-distilled water to the same concentration as the nanoparticles. Sample dilutions were performed as described by the NCCLS [33]. Blank paper disks with diameter of 6.0 mm were impregnated with 25 μL AgNP stock solution. About 20 μL 1.25 mg/mL 3-(4,5-dimethylthiazol-2-yl)-2,5-diphenyltetrazolium bromide (MTT; Sigma-Aldrich) was added to each plate and observed for purple coloration after incubation at 37 °C for 30 min, which indicates microbial growth [34]. The plates were incubated for 24 h at 37 °C for bacteria and for 48 h at 30 °C for fungi. Control experiments were carried out under similar conditions using commercially available antibacterial (streptomycin) or antifungal drug (ketoconazole) as positive control, while 100 % dimethyl sulfoxide was used as negative control. The sensitivity of the microorganism species to the samples was determined by measuring the size of the inhibition zone (including the diameter of the disk) on the agar surface around the disks, with values <6 mm considered to indicate inactivity against the microorganism. Inhibition zones were recorded in millimeters, and the experiment was repeated twice. Experimental results are given as mean ± standard deviation (SD) of the two parallel measurements, and analysis of variance (ANOVA) was performed. Significant differences between means were determined by Duncan's multiple-range test. P values <0.05 were regarded as significant.

Minimum inhibitory concentration (MIC)

A minimum inhibitory concentration study for LX-AgNPs was performed using the broth dilution method [35] using a 96-well microtiter plate format. Different concentrations within the range of 15–100 μg/mL were prepared from 100 μg/mL stock solution of silver nanoparticles using DMSO as diluent. Inocula were prepared by making a direct broth suspension of isolated microbial colonies and adjusting them to achieve turbidity equivalent to a 0.5 McFarland turbidity standard. The suspension in the tube finally contained 10^6 colony-forming units (CFU)/mL of the test organism. Each well of the microtiter plate (96 wells) was filled with 100 μL nutrient broth, 20 μL of 10^6 CFU/mL of the test organism, and 80 μL of different concentrations of AgNPs ranging from 15 to 100 μg/mL. Control wells were filled with broth only or broth and test organisms only. After 24 h of incubation at 37 °C for bacterial strains and 48–72 h at 30 °C for fungi, 20 μL 1.25 mg/mL 3-(4,5-dimethylthiazol-2-yl)-2,5-diphenyltetrazolium bromide (MTT; Sigma-Aldrich) was added to each well and observed for purple coloration after incubation at 37 °C for 30 min, which indicates microbial growth [32]. The minimum concentration of AgNPs that did not show any color change in the wells was recorded as the MIC. The method was replicated three times to validate the results.

Results and discussion

Synthesis

Addition of aqueous leaf extract of *L.* × *intermedia* to 1 mM $AgNO_3$ solution in 1:5 ratio resulted in yellowish brown solution after about 2 min of reaction time. The emergence of color in the solution is due to excitation of surface plasmon resonance (SPR) of conducting electrons in the AgNPs.

UV–Vis spectroscopy

UV–Vis spectroscopic analysis is an indirect but efficient method for detecting nanoparticle formation. The progress of the reaction leading to conversion of Ag^+ from $AgNO_3$ to reduced nanosilver was monitored by observing the color change and absorbance maximum peak in the range of 300–800 nm. As the reaction mixture was continually sampled at intervals, a blue-shift from the initial wavelength of 422 to 411 nm after 90 min of reaction time was observed. Gradual reduction of silver ions was recorded during the incubation time, and this is directly correlated with the synthesis rate of LX-AgNPs. As the incubation time was increased from 0 to 90 min, the SPR intensity increased and the yield of LX-AgNPs was also found to be higher (as shown by the intensity) [36, 37].

The UV–Vis spectra also indicated the onset of digestive ripening during the incubation period, introduced by the molecules of the extract, which is a convenient and efficient method for preparation of particles with narrow size distribution, as observed from the blue-shift of the wavelength. This also indicates particle size

reduction and higher energy [38]. As the absorption peak narrows, it is reasonable to assume that the size distribution of the particles also narrows [39]. So, as the range of particles in solution decreased, the absorption became more focused within a specific range, as observed in the spectra presented in Fig. 1. While aggregates are known to cause a red-shift in the absorption spectra, the broadness of the peak is ascribed to the presence of numerous particles of different sizes still in solution [40].

FTIR spectroscopy

The role of the plant extract as a bioreductant was examined by FTIR analysis of both the plant extract and AgNPs. The FTIR spectra of the *L.* × *intermedia* leaf extract and LX-AgNPs are shown in Fig. 2a and b, respectively. The FTIR spectra show significant changes after the bioreduction process. The spectrum of the leaf extract (Fig. 2a) shows a peak in the range around 1026 cm^{-1}, which is related to C–O bond [41, 42]. The peak around 1461 cm^{-1} can be ascribed to symmetric stretching vibrations of –COO group in the plant extract. The presence of C=O of carbonyl group is confirmed by the distinct peak around 1729 cm^{-1}. This peak, which was found to be enhanced in the spectrum of the nanoparticles, may be due to presence of carbonyl group of esters, which may be in conjunction with a double bond or aromatic ring [43]. Two bands observed at 2918 and 2850 cm^{-1} are ascribed to –CH bonds of alkyl groups, while the strong band at 3659 cm^{-1} may be assigned to –OH of phenolic compounds. The FTIR spectrum of the nanoparticles showed a pattern similar to that of the plant extract, indicating the presence of some

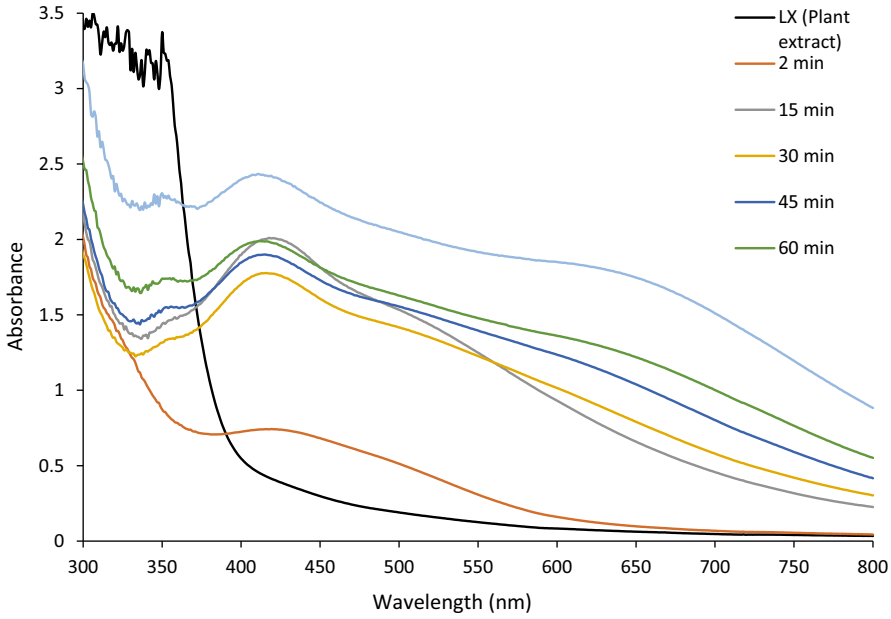

Fig. 1 Surface plasmon resonance exhibited at different intervals during formation of silver nanoparticles mediated by *Lavandula* × *intermedia* (LX-AgNPs)

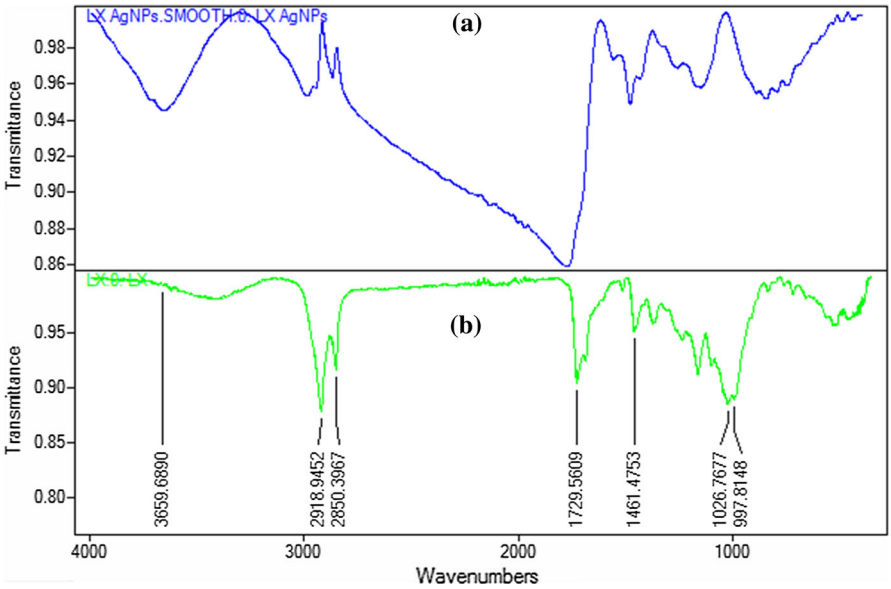

Fig. 2 FTIR spectra of **a** *Lavandula* × *intermedia* leaf powder, **b** LX-AgNPs

phytochemicals from the plant extract. These phytochemicals are responsible for reduction and stabilization of the silver nanoparticles. These FTIR results confirm that plant extract components could possibly have formed a layer covering the metal nanoparticles (i.e., capping of silver nanoparticles) to prevent agglomeration, thereby stabilizing the medium via carbonyl group from esters or essential oils, which are the major components of leaf [44].

Powder X-ray diffraction (PXRD) analysis

The crystalline structure of the synthesized LX-AgNPs was investigated by PXRD analysis. Figure 3 shows the diffraction peaks identified at 44.38°, 51.77°, 76.44°, and 93.11°, corresponding to (1 1 1), (2 0 0), (2 2 0), and (3 1 1) Bragg reflection planes of silver, respectively [45]. These results confirm that the biosynthesized LX-AgNPs had face-centered cubic (fcc) crystalline structure. The result obtained matched with Joint Committee on Powder Diffraction Standards (JCPDS) file no. 04-0783. The intense (1 1 1) reflection compared with the others indicates the growth direction for thin films of Ag [14]. The average crystallite size of LX-AgNPs was estimated from the full-width at half-maximum (FWHM) of the (1 1 1) reflection, as shown in Fig. 3, using the Scherrer formula (1) [46]:

$$D = 0.9\lambda/\beta\cos\theta, \tag{1}$$

where D is the crystallite size, λ is the wavelength of the X-ray source (0.1541 nm), β is the FWHM, and θ is the diffraction angle. The average diameter was obtained as 12.6 nm.

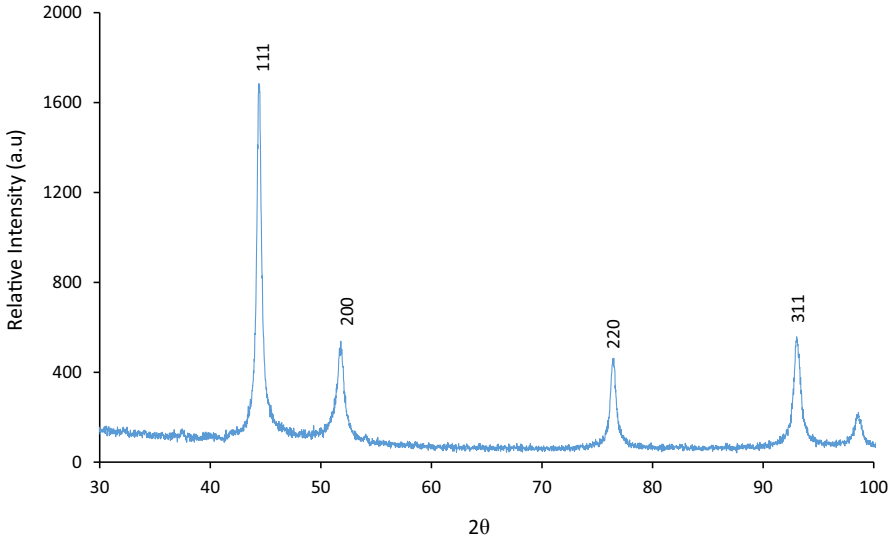

Fig. 3 XRD pattern of LX-AgNPs, indicating face-centered cubic crystal structure

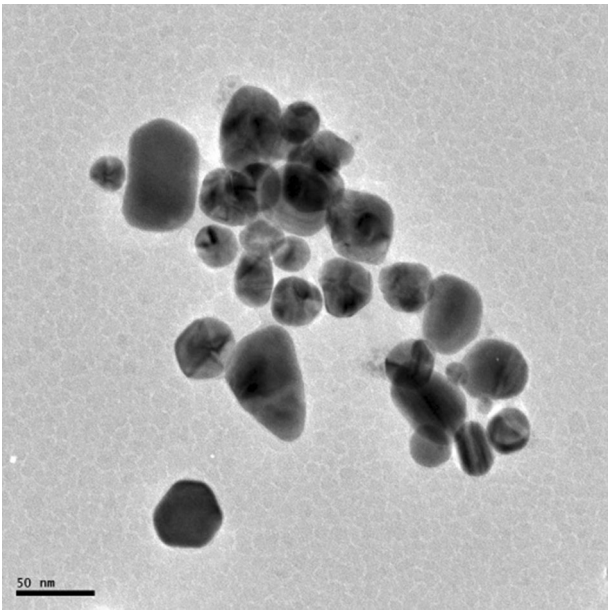

Fig. 4 TEM images of AgNPs formed by reduction of Ag^{+} ions using *Lavandula* × *intermedia* plant extract

Microscopy analysis

Electron microscopy (EM) provides insight into the morphology of the synthesized nanoparticles. The transmission electron microscopy (TEM) image presented in Fig. 4 reveals that the particles were spherical nanoparticles. The primary particle diameter of the TT-AgNPs produced by reducing $AgNO_3$ with the extract ranged from 11 to 47 nm and depended on the components of the extract as well as other factors (temperature, pH, concentration ratio, etc.), as different particle sizes were obtained with different extracts. However, for the larger nanoparticles (i.e., <47 nm), the average crystallite size was found to be less than the particle size, primarily due to multiple-domain diffraction caused by crystal twinning.

Based on our findings, we conclude that the AgNPs synthesized using our approach consist of a mixed population of different crystal structures as well as single-crystalline nanoparticles. They initially exist as a polydispersed system, with dramatic narrowing of the size distribution, culminating in an average particle size of about 12.6 nm, as observed by TEM and supported by the XRD and UV–v is results.

Antimicrobial studies

The broad-spectrum antimicrobial activities of leaf, stalk, and flower extracts of *Lavandula* × *intermedia* have been reported [34]. The antimicrobial data for the LX-AgNPs are presented in Table 1 and Fig. 5. The nanoparticles exhibited larger inhibition zones (in the range of 10–23 mm) compared with *Lavandula* × *intermedia* leaf extract. The FTIR spectrum of the plant extract already confirmed the presence of different constituents such as flavonoids, terpenoids, tannins, and

Table 1 Antimicrobial results for AgNPs and leaf extract of *Lavandula* × *intermedia*

Pathogen	AgNPs	Plant extract	Streptomycin	Ketoconazole	DMSO
Bacillus cereus	18 ± 0.7	13 ± 0.7	20 ± 2.8	—	R
Staphylococcus aureus	19 ± 2.8	11 ± 2.8	22 ± 1.4	—	R
Pseudomonas aeruginosa	19 ± 0.0	12 ± 2.4	24 ± 1.4	—	R
Klebsiella oxytoca	21 ± 0.7	08 ± 0.0	19 ± 0.0	—	R
Escherichia coli	23 ± 0.0	10 ± 0.0	20 ± 0.0	—	R
Proteus mirabilis	10 ± 1.4	R	20 ± 0.7	—	R
Salmonella typhi	17 ± 0.7	08 ± 0.0	23 ± 0.7	—	R
Fusarium oxysporum	15 ± 0.0	08 ± 1.4	—	23 ± 0.0	R
Aspergillus niger	15 ± 0.7	08 ± 1.4	—	21 ± 0.0	R
Candida albicans	18 ± 0.7	R	—	16 ± 1.4	R

Values (in mm) represent the mean of double replications and their standard deviation; standard drugs streptomycin and ketoconazole were used as positive control for antimicrobial studies, (—) means not screened, DMSO was used as negative control and showed no activity, R = resistant. The well diameter was 6 mm, and any activity below 6 mm was considered resistant

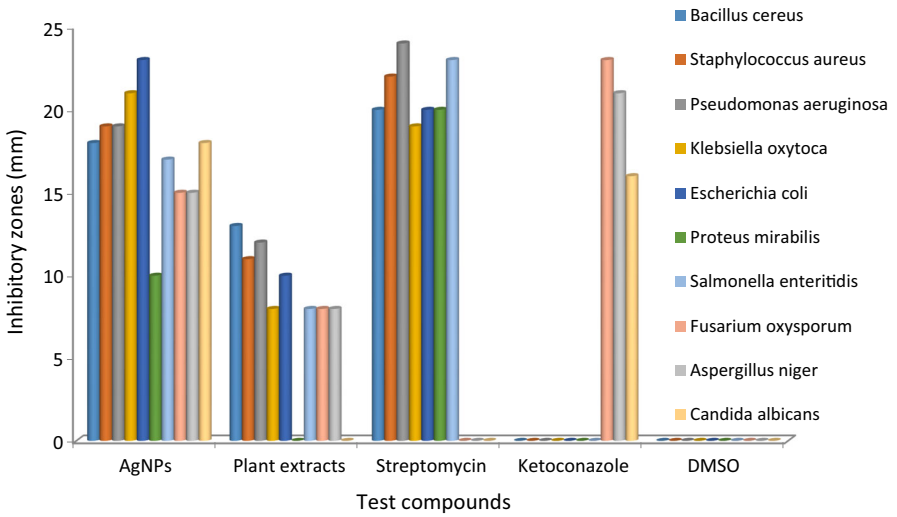

Fig. 5 Histogram representation of antimicrobial results for AgNPs and leaf extract of *Lavandula* × *intermedia*

saponins [34]. The spectrum of the AgNPs showed that these secondary metabolites were also present as stabilizing and capping agents. As a result, some of the constituent metabolites adsorbed onto the silver nanoparticles. The observed enhancement of the antimicrobial activity of the AgNPs compared with the plant extract is due to release of silver ions into microbial cells and also due to the bioactivity of the attached bioactive constituents [47]. Liposolubility could also be the main factor responsible for the increased activity. The lipid membrane around a microbial cell controls its permeability and allows lipid-soluble material into the cell. Chelation decreases the metal ion polarity, due to overlapping of ligand orbital and partial sharing of the positive charge of the metal ion with donor groups. Consequently, there is an increase in the lipophilicity of the complexes which, thus, penetrate the lipid membrane easily and block metal binding sites on enzymes of the microorganisms [48]. Based on this latter point, it can be inferred that the ease of penetration of AgNPs through the cell membrane of Gram-negative bacteria compared with the Gram-positive bacterial cell wall is the reason for the Gram-negative bacteria being more susceptible to the AgNPs compared with the Gram-positive bacteria.

Due to the significant antimicrobial activities of the AgNPs at concentration of 100 µg/mL against the pathogens (Table 1), they were further screened at lower concentrations to determine the minimum inhibitory concentration (MIC) against the microbes. The MIC values were lowest for *K. oxytoca*, *Candida albicans*, and *E. coli* at concentration of 15 µg/mL (Table 2). According to these data, the organisms that were highly susceptible to AgNPs also exhibited low MIC values, reflecting their potential as microbial inhibitors.

Table 2 MIC values of silver nanoparticles (AgNPs)

Microbial strain	MIC (μg/mL)
Bacillus cereus	50
Staphylococcus aureus	25
Pseudomonas aeruginosa	25
Klebsiella oxytoca	15
Escherichia coli	15
Proteus mirabilis	50
Salmonella typhi	25
Fusarium oxysporum	25
Aspergillus niger	25
Candida albicans	15

Conclusions

Biosynthesis of AgNPs using *Lavandula* × *intermedia* leaf extract is reported. The nanoparticles were characterized for their structural and morphological properties. UV–v is spectroscopy showed maximum absorption for the AgNPs at 422 nm after 2 min of reaction, with a blue-shift to 411 nm after 90 min of reaction. TEM and XRD studies revealed that the AgNPs were spherical in shape with average particle size of 12.6 nm. The FTIR spectrum of the AgNPs revealed the presence of secondary metabolite constituents from the plant. Hence, the plant extract not only reduced the silver particles, but also served as a stabilizing and capping agent. Furthermore, the AgNPs exhibited better antimicrobial properties against the screened pathogens compared with leaf extract of *Lavandula* × *intermedia*. The antimicrobial properties of the AgNPs against the tested microbes compared favorably with streptomycin and ketoconazole. We report a safe, fast, and environmentally safe process for synthesis of bioactive silver nanoparticles.

Acknowledgments E.E.E. acknowledges North West University Mafikeng campus, South Africa for offering him a Postdoctoral Research position and for providing the facilities necessary to carry out this work.

References

1. S.N. Kharat, V.D. Mendhulkar, Mater. Sci. Eng. C **62**, 719–724 (2016)
2. S. Mohan, O.S. Oluwafemi, S.P. Songca, V.P. Jayachandran, D. Rouxel, O. Joubert, N. Kalarikkal, S. Thomas, J. Mol. Liq. **213**, 75–81 (2016)
3. D. Cruz, P.L. Falé, A. Mourato, P.D. Vaz, M.L. Serralheiro, A.R.L. Lino, Coll. Surf. B Biointerfaces **81**, 67–73 (2010)
4. P.M. Mishra, S.K. Sahoo, G.K. Naik, K. Parida, Mater. Lett. **160**, 566–571 (2015)
5. X.R. Song, N. Goswami, H.H. Yang, J. Xie, Analyst **11**, 3126–3140 (2016)
6. S. Gul, M. Ismail, M.I. Khan, S.B. Khan, A.M. Asiri, I.U. Rahman, M.A. Khan, M.A. Kamboh, Asian Pac. J. Trop. Dis. **6**, 311–316 (2016)
7. V. Dhand, L. Soumya, S. Bharadwaj, S.C. Chakra, D. Bhatt, B. Sreedhar, Mater. Sci. Eng. **58C**, 36–43 (2016)
8. P.M. Mishra, S.K. Sahoo, G.K. Naik, K. Parida, Mater. Lett. **160**, 566–571 (2015)
9. M.J. Ahmed, G. Murtaza, A. Mehmood, T.M. Bhatti, Mater. Lett. **153**, 10–13 (2015)

10. N.H. Rao, N. Lakshidevi, S.V.N. Pammi, P. Kollu, S. Ganapaty, P. Lakshmi, Mater. Sci. Eng. C **62**, 553–557 (2016)
11. J.L. Lopez-Miranda, M. Vazquez, N. Fletes, R. Esparza, G. Rosas, Mater. Lett. **176**, 285–289 (2016)
12. R.P. Raman, S. Parthiban, B. Srinithya, V.V. Kumar, S.P. Anthony, A. Sivasubramanian, M.S. Mulhuraman, Mater. Lett. **160**, 400–403 (2015)
13. A. Miri, M. Sarani, M.R. Bazaz, M. Darroudi, Spectrochim. Acta **141**, 287–291 (2015)
14. M. Ghaedi, M. Yousefinejad, M. Safapoor, H.Z. Khafri, M.K. Purkait, J. Ind. Eng. Chem. **31**, 167–172 (2015)
15. B. Shan, Y. Cai, M. Sun, H.J. Corke, Agric. Food Chem. **53**, 7749–7759 (2005)
16. L.T. Claveria, O. Jauregui, J. Bastida, C. Codina, F. Viladomat, J. Agric. Food Chem. **55**, 8436–8443 (2007)
17. C. Jianu, G. Pop, A.T. Gruia, F.G. Horhat, Int. J. Agric. Biol. **15**, 772–776 (2013)
18. C.R. Flores, A. Pennec, C. Nugier-Chauvin, R. Daniellou, L. Herrera-Estrella, A.L. Chauvin, J. Mex. Chem. Soc. **58**, 452–455 (2014)
19. S.G. Deans, Antimicrobial properties of lavender volatile oil, in *Lavender: the genus Lavandula*, ed. by M. Lis-Balchin (CRC Press, London, 2002), p. 171
20. T. Moon, J.M. Wilkinson, H.M.A. Cavanagh, Int. J. Aromather. **16**, 9–14 (2006)
21. K. Bayoub, T. Baibai, D. Mountassif, A. Retmane, A. Soukri, Afr. J. Biotechnol. **9**, 4251–4258 (2010)
22. B. Blazekovic, G. Stanic, S. Pepeljnjak, S. Vladimir-Knezevic, Molecules **16**, 4241–4253 (2011)
23. F. Giraud, R. Guillon, C. Logé, F. Pagniez, C. Picot, M.L. Borgne, L.P. Pape, Bioorgan. Med. Chem. Lett. **19**, 301–304 (2009)
24. M.M. Patel, L.J. Patel, Sci. World J. **2014**, 1–10 (2014)
25. N. Raman, A. Sakthivel, K. Rajasekaran, Mycobiology **35**, 150–153 (2007)
26. G. Kumar, D. Kumar, S. Devi, R. Verma, R. Johari, Int. J. Eng. Sci. Technol. **3**, 1630–1635 (2011)
27. S. Prabhu, E.K. Poulose, Int. Nano Lett. **2**, 1–10 (2012)
28. L. Berkovich, G. Earon, I. Ron, A. Rimmon, A. Vexler, S. Lev-Ari, BMC Complement. Altern. Med. **13**, 212 (2013)
29. A.U. Khan, Y. Wei, A. Ahmad, Z.U. Khan, K. Tahir, S.U. Khan, N. Muhammad, F.U. Khan, Q. Yuan, J. Mol. Liq. **215**, 39–46 (2016)
30. W.A. McCracken, R.A. Cowsan, *Clinical and Oral Microbiology* (Hemisphere, New York, 1983), p. 512
31. R. Chandrasekaran, S. Gnanasekar, P. Seetharaman, R. Keppanan, W. Arockiaswamy, S. Sivaperumal, J. Mol. Liq. **219**, 232–238 (2016)
32. B. Fernández-Torres, I. Inza, J. Guarro. Antimicrob. Agents Chemother. **49**(5), 2116–2118 (2005). doi:10.1128/AAC.49.5.2116-2118
33. National Committee for Clinical Laboratory Standards. 2002. Reference method for broth dilution antifungal susceptibility testing of yeasts. Approved standard M27-A2. National Committee for Clinical Laboratory Standards, Wayne, PA
34. H.J. Simon, E.J. Yin, Appl. Microbiol. **19**, 573–579 (1970)
35. I. Wiegand, K. Hilpert, R.E. Hancock, Nat. Protoc. **3**(2), 163–175 (2008). doi:10.1038/nprot.2007.521
36. S. Rajeshkumar, C. Malarkodi, M. Vanaja, G. Annadurai, J. Mol. Struct. **1116**, 165–173 (2016)
37. G. Sathishkumar, C. Gobinath, K. Karpagam, V. Hemamalini, K. Premkumar, S. Sivaramakrishnan, Col. Surf. B Biointerfaces **95**, 235–240 (2012)
38. A. Verma, M.S. Mehata, J. Radiat. Res. Appl. Sci. **9**, 109–115 (2016)
39. A.B. Smetana, K.J. Klabunde, L.M. Sorensen, J. Colloids Interface Sci. **284**, 521–526 (2005)
40. B.L.V. Prasad, S.I. Stoeva, C.M. Sorensen, K.J. Klabunde, Langmuir **18**, 7515 (2002)
41. J. Huang, Q. Li, D. Sun, Y. Lu, Y. Su, X. Yang, Nanotechnology **18**, 105104–105115 (2007)
42. B. Ankamwar, M. Chaudhary, M. Sastry, Synth. React. Inorg. Met-Org. Nano-Met. Chem. **35**, 19–26 (2005)
43. W. Kemp, In: *Organic spectroscopy* (Macmillan, London, 1991)
44. B. Sadeghi, F. Gholamhoseinpoor, Spectrochim. Acta **134A**, 310–315 (2015)
45. R. Sarkar, P. Kumbhakar, A.K. Mitra, Dig. J. Nanomater. Biostruct. **5**, 491–496 (2010)
46. A. Miri, M. Sarani, M.R. Bazaz, M. Darroudi, Spectrochim. Acta **141A**, 287–291 (2015)
47. A.C. Ekennia, D.C. Onwudiwe, C. Ume, E.E. Ebenso, Bioinorg. Chem. Appl. **2015**, 1–10 (2015)
48. A. Phull, Q. Abbas, A. Ali, H. Raza, S. kim, M. Zia, I.U. Haq., Future J. Pharm. Sci. (2015). doi:10.1016/j.fjps.2016.03.001